

Properties of In-cirrus Contrails from Airborne Remote-sensing Data

Mahshad Soleimanpour ^(a), Silke Groß ^(b), and Matthias Tesche ^(a)

(a) Leipzig Institute for Meteorology (LIM), Leipzig University, Leipzig, Germany

(b) Institut für Physik der Atmosphäre, Deutsches Zentrum für Luft- und Raumfahrt (DLR), Oberpfaffenhofen, Germany

mahshad.soleimanpourboroujeni@uni-leipzig.de

Abstract: Aviation impacts the Earth's energy balance through non-CO₂ effects and emissions of exhaust gases and soot. Planes flying through cirrus clouds can create contrails that might affect the climate effect of these clouds. In this study, we aim to quantify the impact of such embedded contrails based on active remote-sensing observations with the German research aircraft HALO. WALES lidar observations during the ML-CIRRUS campaign indicate that embedded contrails could be identified by a particle backscatter coefficient larger than 4 Mm⁻¹ sr⁻¹ and a particle linear depolarization ratio below 46%. In contrast, cases that don't fulfil these conditions are considered as unperturbed cloud. Identified candidates for embedded contrails are linked to the passage of individual aircrafts for verification. The goal is to detect embedded contrails in WALES observations and to quantify their optical and microphysical characteristics.

1. Introduction

Aviation has a significant impact on the Earth's energy balance. In addition to the release of exhaust gases and soot, it is known to have various non-CO₂-related effects [7]. The formation of linear contrails and contrail cirrus is one of the most notable effects, which can be observed through passive remote-sensing techniques from space [8].

It has been observed that optically thin cirrus and contrails have a warming effect on the atmosphere [1-6]. The radiative effect of contrails and cirrus clouds formed in clear air has been extensively studied, e.g., by including them as a separate cloud class in global climate models [1] and coupling contrail cirrus simulations with re-analysis data [10].

Little research has been conducted on the effects of aircraft flying through existing cirrus clouds. The resulting embedded contrails are created when freshly formed contrails overlap with natural cirrus clouds [4]. Embedded contrails, before the removal of the contrail ice via aggregation within a few hours after formation, can cause a local decrease in the ice crystal effective radius (ICER), as well as a local increase in mean ice crystal number concentration (ICNC) and extinction coefficient when compared to the unperturbed cloud [4]. This also leads to an increase in cloud optical thickness (COT), which could potentially

shift the cloud's climate impact from net warming to net cooling [17].

Observational studies of contrails and contrail cirrus are mostly based on passive spaceborne remote-sensing measurements [3,8]. These measurements provide important properties such as COT, but they are limited in that they cannot reveal what is happening within a cloud. To get a better understanding of the internal structure of cirrus clouds, active remote sensing with lidar is used. This method enables height-resolved measurements that can be used to obtain the base and top heights of cirrus clouds, as well as to derive profiles of their optical and microphysical properties [5].

In this study, embedded contrails are detected from active remote-sensing observations performed with the German research aircraft HALO during ML-CIRRUS. The verified contrails will be studied to analyze the properties of embedded contrails, including their optical and microphysical characteristics.

2. Methods

The HALO mission ML-CIRRUS was specifically conducted to explore cirrus clouds in mid-latitudes [15], employing both in-situ instruments and active remote sensing through the WALES lidar [16]. Lidar measurements capture the particle backscatter coefficient $\beta(\lambda)$, which increases with a growing number of scatterers.

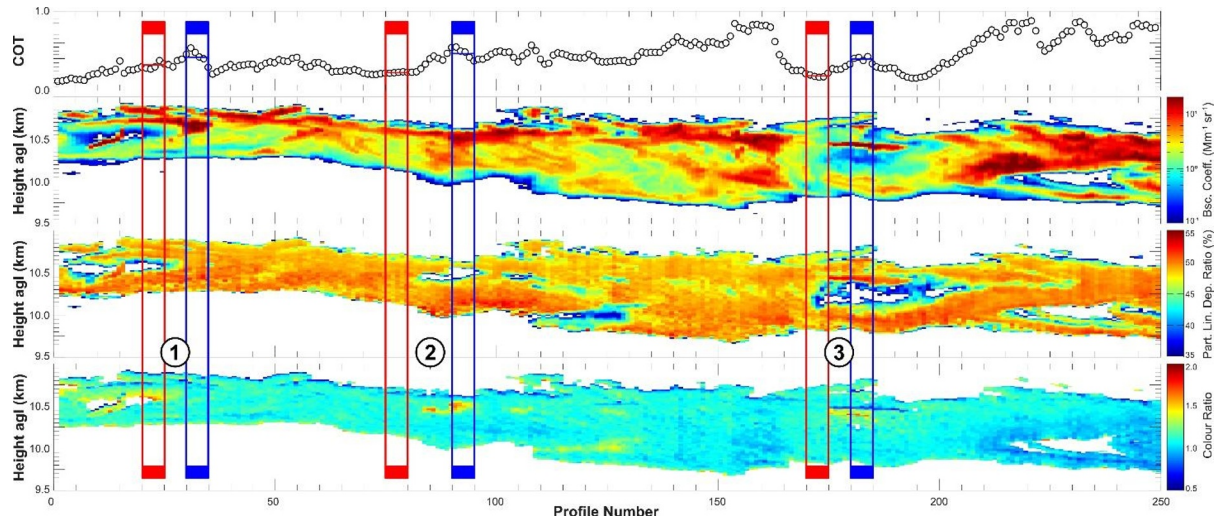


Figure 1. Four minutes of WALES lidar observations of a cirrus over southwestern Germany around 1554 UTC on 10 April 2014 during ML-CIRRUS in form of COT, β , and δ at 532 nm, and CR as the ratio of β at 532 and 1064 nm. Blue boxes highlight increased COT and inhomogeneities that could represent embedded contrails. Red boxes mark unperturbed parts of the clouds in close vicinity.

The color ratio $CR = \beta(\lambda_1)/\beta(\lambda_2)$, indicates changes in the backscatter coefficient with wavelength, amplifying as the scatterer size decreases. Additionally, the particle linear depolarization ratio $\delta(\lambda)$ is evaluated, showing sensitivity to both scatterer size and shape [11]. In this context, the identified backscatter signal emanates from ice crystals within cirrus clouds. Vertical integration of $\beta(\lambda)$ across the height span of a cirrus cloud and multiplication with a lidar ratio of 20 sr for cirrus gives the cloud optical thickness (COT).

Inhomogeneities in cirrus clouds with embedded contrails should show more ice crystals (increased ICNC) which would have a smaller size (decreased ICER). Lidar measurements would indicate these in the form of increased β , COT, and CR, as well as decreased δ . The analysis of airborne remote-sensing data during HALO campaigns in busy air-traffic areas is complemented by commercial data on the position of individual aircraft to allow for the verification of identified contrails in cirrus clouds.

3. Results

We propose a method for the identification of embedded contrails in lidar observations that considers the parameters COT, β , CR, and δ . Figure 1 presents about four minutes of WALES lidar measurements of a cirrus over southwestern Germany during ML-CIRRUS at 1554 UTC on 10 April 2014. The identification of the three indicated potential contrail perturbances and their adjacent unperturbed reference regions involves

considering areas with an elevated COT [12] as well as in the profiles of the available parameters.

Case 2 stands out as the main candidate for embedded contrails after reviewing all three cases. The combination of a peak in β , a significant drop in δ , and a clear increase in CR compared to the unaffected background suggests the presence of small ice crystals from a contrail's vortex. This observation is in line with both lidar measurements [14] and high-resolution contrail modeling [13].

Verification of embedded contrails requires considering information about air traffic in the regions where lidar measurements are taken. Hence, aircraft position data for confirming intercepts between the flight tracks of HALO and other aircraft was procured from Flightradar24.

Figure 2 displays the matching results of commercial aircraft positions in a grid box from 5°E, 49°N to 9°E, 50°N on 10 April 10 2014 with the HALO flight of the same day. The highlighted section of the HALO track in the inset aligns with the details in Figure 1. The examination suggests that the cirrus disturbance, observed at profiles 90 to 95, is likely attributable to the passage of flight AF1808 from Paris to Stuttgart, crossing the HALO flight track close to this location.

The knowledge acquired by examining the scenarios in Figure 1 and linking case 2 to the real-time passage of an aircraft is employed to establish an initial mask for identifying embedded contrails using WALES lidar measurements.

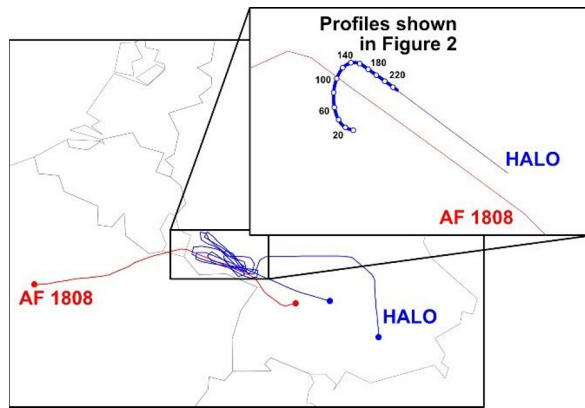


Figure 2. Flight track of HALO (blue) and Air France flight AF1808 from Paris to Stuttgart (red). Circles denote profile numbers at intervals of 20.

The 2D histogram in Figure 3 indicates that the majority of lidar time-height bins in Figure 1 are characterized by either low β and varying δ or a δ around 50% with varying β . A small number of instances corresponding to a combination of rising β values and declining δ values form a third branch that is considered to be related to embedded contrails.

Figure 3 also includes results of profiles averaged over the boxes in Figure 1. Only the mean of profiles 90 to 95, specifically the perturbed profile of case 2 connected to flight AF1808, shows a different parameter combination compared to the branches around $\beta = 0 \text{ Mm}^{-1} \text{ sr}^{-1}$ and $\delta = 50\%$. This suggests that embedded contrails might be detectable through a simple threshold-based method with $\beta > 4 \text{ Mm}^{-1} \text{ sr}^{-1}$ and $\delta < 46\%$ while other cases represent unperturbed cloud.

The application of the suggested detection mask is presented in Figure 4. It indicates that only the

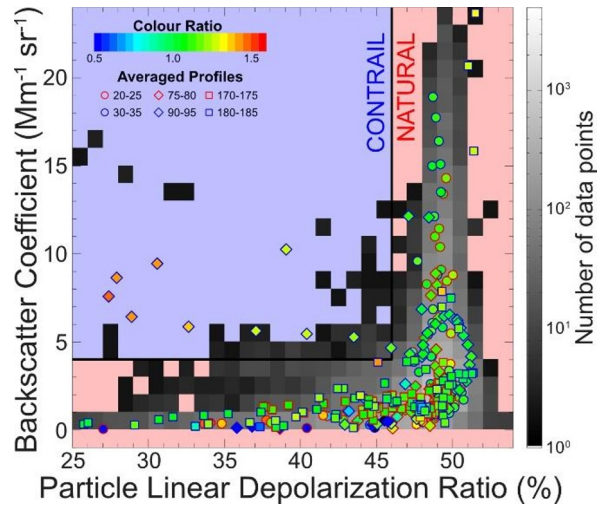


Figure 3. 2D-histogram (grayscale) of β and δ based on the individual profiles in Figure 1 and scatter plot of β and δ (circles) for the average profiles according to the blue and red boxes in Figure 1. The circle shading indicates the CR. Red and blue areas mark regions of unperturbed cloud and embedded contrail, respectively.

perturbation of case 2 shows features that are in line with the criteria of identifying embedded contrails. In addition, the detection mask reveals further potential instances of embedded contrails that warrant closer inspection. In future, the detection mask will be refined using a larger set of ML-CIRRUS observations and flight-track data. The embedded contrails identified with the thus refined detection mask also during other HALO flight campaigns will be studied for the optical properties. The combination of WALES with airborne cloud radar measurements during dedicated HALO campaigns furthermore enables the retrieval of ICER and ICNC. These observations will be used in combination with the

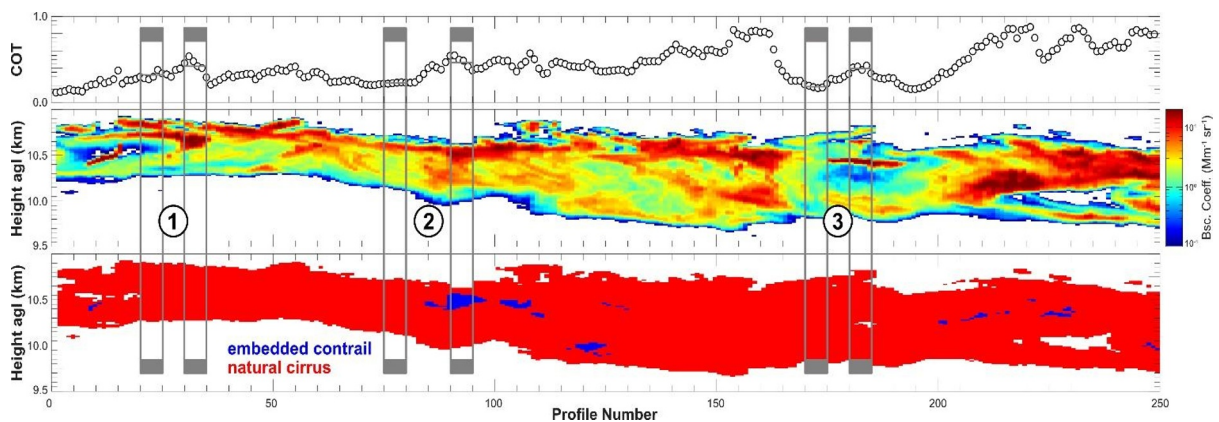


Figure 4. Same as Figure 1 but showing the results of masking regions with $\beta > 4 \text{ Mm}^{-1} \text{ sr}^{-1}$ and $\delta < 46\%$ as embedded contrails (blue) compared to the unperturbed cirrus (red) following the detection scheme in Figure 3.

detection of embedded contrails to also characterize the microphysical properties of perturbed cirrus clouds.

4. Conclusion

Aviation significantly influences Earth's energy balance not only through CO₂ emissions but also by generating contrails that might evolve into longer-lasting cirrus clouds or form in cirrus to begin with. We use WALES measurements conducted during the ML-CIRRUS campaign with the German research aircraft HALO to develop a method for identifying embedded contrails. The method is based on threshold values of the particle backscatter coefficient and the particle linear depolarization ratio. The findings allow for the selection of candidates for embedded contrails, facilitating further research into their optical and microphysical properties, contributing to a more comprehensive understanding of aviation's impact on the atmosphere.

5. References

- [1] Bock and Burkhardt, "Reassessing properties and radiative forcing of contrail cirrus using a climate model", *JGR* **121**, [2016JD025112](#) (2016).
- [2] Boucher, "Air traffic may increase cirrus cloudiness", *Nature* **397**, [10.1038/16169](#) (1999).
- [3] Duda et al., "Estimation of 2006 Northern Hemisphere contrail coverage using MODIS data", *GRL* **40**, doi:[grl.50097](#) (2013).
- [4] Gierens, "Selected topics on the interaction between cirrus clouds and embedded contrails", *ACP* **12**, [acp-12-11943-2012](#) (2012).
- [5] Iwabuchi et al., "Physical and optical properties of persistent contrails: Climatology and interpretation", *JGR* **117**, [2011JD017020](#) (2012).
- [6] Kärcher, "Cirrus Clouds and Their Response to Anthropogenic Activities", *Curr. Clim. Change Rep.* **3**, [s40641-017-0060-3](#) (2017)
- [7] Lee et al., "Aviation and global climate change in the 21st century", *Atmos. Environ.* **43**, [j.atmosenv.2009.04.024](#) (2009).
- [8] Minnis et al., "Linear contrail and contrail cirrus properties determined from satellite data", *GRL* **40**, [grl.50569](#) (2013).
- [9] Sassen, "Contrail-Cirrus and Their Potential for Regional Climate Change", *BAMS* **78**, [1520-0477\(1997\)078<1885:CCATPF>2.0.CO;2](#) (1997).
- [10] Schumann and Graf, "Aviation-induced cirrus and radiation changes at diurnal timescales", *JGR* **118**, [jgrd.50184](#) (2013).
- [11] Tesche et al., "Vertical profiling of Saharan dust with Raman lidars and airborne HSRL in southern Morocco during SAMUM", *Tellus* **61B**, [j.1600-0889.2008.00390.x](#) (2009).
- [12] Tesche et al., "Aviation effects on already-existing cirrus clouds", *Nature Comms.* **7**, [ncomms12016](#) (2016).
- [13] Unterstrasser, "Properties of young contrails – a parametrisation based on large-eddy simulations", *ACP* **16**, [acp-16-2059-2016](#) (2016).
- [14] Urbanek et al., "High depolarization ratios of naturally occurring cirrus clouds near air traffic regions over Europe", *GRL* **45**, [2018GL079345](#) (2018).
- [15] Voigt et al., "ML-CIRRUS: The Airborne Experiment on Natural Cirrus and Contrail Cirrus with the High-Altitude Long-Range Research Aircraft HALO", *BAMS* **98**, [BAMS-D-15-00213.1](#), (2017).
- [16] Wirth et al., "The airborne multi-wavelength water vapor differential absorption lidar WALES: system design and performance", *Appl. Phys. B* **96**, [s00340-009-3365-7](#) (2009).
- [17] Zhang et al., "Effect of crystal size spectrum and crystal shape on stratiform cirrus radiative forcing", *Atmos. Res.* **52**, [S0169-8095\(99\)00026-5](#) (1999).